RESEARCH REPORT

Hurricane Occurrence Along the U.S. Gulf and Atlantic Coasts, 1900-2025

An updated point climatology with three occurrence definitions, resampling uncertainty on the rankings, ENSO stratification, and a modern wind-field cross-check

Abstract

Point-based climatologies of tropical cyclone strikes along the U.S. Gulf and Atlantic coasts (Simpson and Lawrence 1971; Elsner and Kara 1999; Keim et al. 2007) have identified three regions of concentrated hurricane activity: south Florida, the Outer Banks of North Carolina, and the north-central Gulf Coast. We update this climatology through the 2025 season using the HURDAT2 best-track record, evaluated continuously along the coast on a 33,916-point mesh under three explicit occurrence definitions: hurricane-strength coastline crossings within 50 n mi (L50), hurricane centers passing within 50 n mi (H50), and major-hurricane centers within 50 n mi (M50). Under a common 1900-2025 window the three focal points are recovered under all three definitions. A site-by-site comparison with Keim et al. (2007) over their 1901-2005 window gives rank agreement of 0.84-0.88 (Spearman) at every intensity tier, with our symmetric center-proximity intervals shorter than their asymmetric-swath values by a factor that grows with intensity (median 0.90, 0.70, 0.60), a gradient the two constructions predict; against NHC's HURISK-modeled 50 n mi return periods, which count the same event as our H50, the empirical intervals run about 0.74 of the modeled values on every window tested, with rank order preserved. Which focal point leads depends on the definition: south Florida under L50 and M50, the Outer Banks under H50. Season-block bootstrap with re-optimization gives the leading region 63-69% support in resamples; adding era-dependent perturbation of landfall positions, which reach ~60 n mi before 1944, lowers the crossing-metric leader's support to 45% against 28% for southeast Louisiana, so we report most-probable maxima rather than winners and rest the south Florida result on its convergence across radii and definitions. Annual counts at south Florida are overdispersed, reflecting a documented tendency toward multi-hurricane seasons with direct bearing on preparedness. Stratifying 1950-2025 by NOAA's Relative Oceanic Niño Index reproduces the phase structure of Bove et al. (1998): La Niña seasons show twice the strict landfall rate of El Niño seasons (rate ratio 2.00; exact 95% CI 1.14-3.61). For 2004-2025, presence inside the analyzed hurricane-force wind envelope shows no unique maximum. Results are occurrence climatology, not risk; code and data are published.

1. Introduction

Where along the U.S. coast have hurricanes arrived most often, and how sure can that ranking be? The question has a lineage. Simpson and Lawrence (1971) computed strike frequencies for 80-km coastal segments from 1886-1970; Ho et al. (1975, 1987) produced and then updated NOAA's own 50 n mi coastal-interval climatology, decomposing occurrence into entering, exiting, and alongshore storms and, in the 1987 revision, naming the Mississippi Delta, south Florida, Cape Hatteras, and Cape Cod as protrusions that generalized coastal analysis cannot represent; Elsner and Kara (1997, 1999) computed county-level return periods for 1900-1996; and Keim, Muller, and Stone (2007), extending Muller and Stone (2001), analyzed 105 years of tropical storm and hurricane strikes at 45 coastal sites from Brownsville, Texas, to Eastport, Maine, and found "three focal points for activity": south Florida, the Outer Banks of North Carolina, and the north-central Gulf Coast. The National Hurricane Center's return-period products, built on the HURISK program that grew out of NHC's climatology work of the late 1960s and was documented by Neumann (1987), and tabulated in Blake et al. (2011), identify the same regions.

Since then the field has largely moved from unconditional descriptive point climatologies to conditional and simulation-based models: covariate count models at county or cluster scale (Jagger et al. 2001; Kozar et al. 2012; Villarini et al. 2012), statistical track models that ask whether local counting is the right approach at all (Hall and Jewson 2007, 2008), and a hierarchical Bayesian treatment that infers the pooling a fixed radius imposes (Tolwinski-Ward 2015). No unconditional point climatology of the whole coast has been published since Keim et al. (2007). The intervening seasons include 2004-2005, 2017-2022, and 2024, among the most active landfall periods in the record; the HURDAT2 reanalysis has revised the early record (Landsea and Franklin 2013); systematic quadrant wind radii now span more than twenty seasons; and NOAA has adopted a new ENSO index, the Relative Oceanic Niño Index (RONI), for operational classification. This report updates the descriptive point climatology through 2025 and addresses three questions the earlier work left open or could not yet ask.

First, each earlier climatology fixed a single event definition. Simpson and Lawrence counted strikes on fixed 80-km coastal segments; Keim et al. modeled storm reach with an asymmetric swath of assumed width; NHC's products and Ho et al. count centers passing within 50 n mi. We compute three definitions on one common mesh, from a strict coastline-crossing catalogue to center proximity to major-hurricane center proximity, and show which conclusions depend on the definition and which do not.

Second, none of the earlier point climatologies quantified the uncertainty of the *ranking*: a maximum selected from many coastal points is biased upward, and the pointwise interval at that point does not say whether it leads its neighbors. We resample seasons and perturb landfall positions by their era-dependent uncertainty, re-locating the maximum on each replicate and reporting how often each region wins.

Third, the record now supports two cross-checks that the earlier work could not make: an ENSO stratification of the landfall series that revisits Bove et al. (1998) with 28 more seasons and the current index, and a direct wind-envelope exposure count from analyzed wind radii for 2004-2025.

A descriptive climatology of this kind is the object that both neighboring research traditions consume rather than compete with. Seasonal landfall forecasts scale a constant-rate climatology by predicted activity: the Colorado State University forecasts derive their landfall probabilities from Poisson fits to storms tracking within 50 miles of each landmass, which is this report's H50 and M50 construct. Synthetic-track hazard models validate their simulated crossing rates against the observed record. Neither branch produces the historical count itself, and neither has done so on the current record.

The results are occurrence climatology. They describe where and how often hurricane conditions have arrived; they do not combine surge, rainfall, exposure, or vulnerability, and they should not be read as a ranking of risk.

2. Data

Best-track record. The meteorological basis is the North Atlantic HURDAT2 best-track archive (Landsea and Franklin 2013), current through the 2025 season, accessed through NOAA/NCEI IBTrACS v04r01 (Knapp et al. 2010), from which we use only the U.S.-agency fields and main tracks: positions, six-hourly maximum sustained winds, storm status, landfall markers, and, from 2004, quadrant wind radii.

Landfall catalogue. HURDAT2 "L" records mark the intersection of the surface center with a coastline, NHC's definition of landfall. The strict catalogue keeps L records at hurricane status with winds of at least 64 kt, restricted to the continental United States and the Florida Keys. The machine-readable L markers are documented as complete for 1851-1945 and from 1991 onward (Landsea and Franklin 2013); the reanalysis has since supplied them for 1946-1970, leaving a residual gap in 1971-1990. We reconstructed the affected crossings from adjacent best-track positions, land-distance fields, and the NOAA/AOML chronology of continental U.S. hurricanes, as Klotzbach et al. (2018) did for the same gap; the reconstruction added twelve hurricane crossings from eleven storms in 1971-1982, matching the AOML chronology entry for entry, while the existing markers for 1983-1990 already agreed with the chronology. One deliberate divergence: the chronology lists Fern (1971) as a Category 1 Texas landfall, but the best-track wind at the crossing is 60 kt, and the strict rule excludes it. The catalogue contains 376 landfall rows across 296 storms; a storm with two qualifying crossings contributes two rows but counts once at any given location.

ENSO classification. Seasonal phase uses NOAA's Relative Oceanic Niño Index, adopted by the Climate Prediction Center for operational ENSO monitoring in February 2026. Following NOAA's convention, an event requires five consecutive overlapping seasons at or beyond ±0.5°C, and each hurricane season is assigned the phase of its August-September-October value. This yields 20 El Niño, 20 La Niña, and 36 neutral seasons in 1950-2025. The 2025 season falls in the La Niña set on the RONI values available at analysis; NOAA's classification of the 2025-26 event is not final, and NOAA notes that event labels can shift between indices.

Coastal geometry. Coastal candidates use the GSHHS/GSHHG shoreline database (Wessel and Smith 1996) and a high-resolution land-sea mask.

Windows. The record is not uniformly observed. NOAA/AOML's regional reliability estimates place the start of reliable hurricane records near 1880 for Louisiana and northwest Florida and near 1900 for southeast and southwest Florida, and give the reliable period for the U.S. coastline as a whole as 1900 to present. Landsea (2007) takes 1900 as the year from which nearly all tropical cyclones approaching the U.S. coast would have been detected and recorded, Ho et al. (1987) and Elsner and Kara (1997) begin their point and county climatologies in 1900 for the same reason, and Vecchi et al. (2021) adopt the same date. We therefore use 1900-2025 (126 seasons) as the primary window for coastwide comparison, report the full 1851-2025 archive only to show what the truncation changes, use 1950-2025 for ENSO stratification (the RONI record), and 2004-2025 for wind-radii metrics. The choice of 1900 is set by the observing system, not by our results; it is the latest of AOML's regional dates and is forced by south Florida's own record being the sparsest in the table.

The landfall record's suitability for a climatology of this kind rests on evidence that its known inhomogeneities fall mostly on storms that never reached the U.S. coast. The century-scale rise in basin counts is concentrated in short-lived systems of two days or less (Landsea et al. 2010); Chenoweth's (2014) independent documentary compilation of 1851-1898 added roughly 73% to the basin count while changing the net number of U.S. landfalling hurricanes by about 1%; and Vecchi et al. (2021) conclude that the apparent long-term decline in the U.S. share of basin storms is an observing artifact. Two counterweights apply: NOAA/GFDL notes that the landfall record, though more reliable than the basin record, has weaker signal-to-noise properties because it is a smaller sample, and the record of landfall *intensity* is less stable than that of landfall *counts*.

3. Methods

3.1 Occurrence definitions

We evaluate three occurrence definitions on the same coastal mesh, listed from most to least restrictive, and two envelope definitions for the modern record.

Code	Event counted at a location	Window
L50	A hurricane-strength (≥64 kt) coastline crossing within 50 n mi	1900-2025
H50	A hurricane center passing within 50 n mi at ≥64 kt	1900-2025
M50	A hurricane center passing within 50 n mi at ≥96 kt	1900-2025
R64	The analyzed 64-kt wind envelope covers the location	2004-2025
R34	The analyzed 34-kt wind envelope covers the location while the storm is a hurricane	2004-2025

The exposure definitions answer different questions

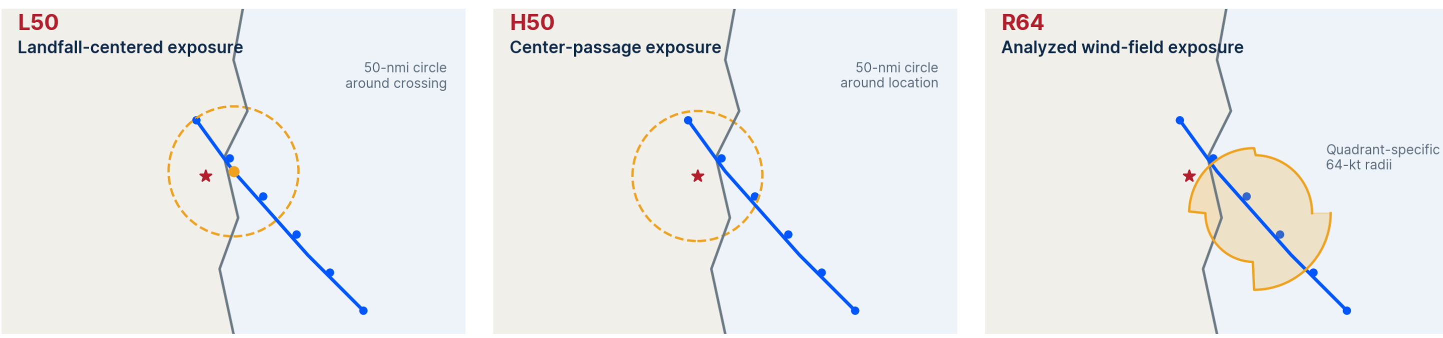

Figure 1. Landfall-centered, center-passage, and wind-field exposure geometries.

Terminology. We follow NHC's definitions where they exist. *Landfall* is the intersection of the surface center with a coastline; our L catalogue uses exactly the HURDAT2 records that mark it. NHC's *strike* is a distinct construct, a 125 n mi diameter circle offset 12.5 n mi to the right of the track, and *direct hit* is defined on the radius of maximum wind; our metrics are neither, and we do not use those terms for them. Keim et al. (2007) also use "strike" for their swath model, which likewise differs from ours (Section 4.2). We say *mean interval* rather than *return period* to mark that our figures are empirical counts over a fixed window, whereas NHC's published return periods are model estimates. Units follow the source record: winds in knots (1 kt = 0.514 m s^{-1}) and distances in nautical miles (1 n mi = 1.852 km), so that every figure is directly comparable with the official products.

3.2 The radius: a stated position

Any location-specific climatology requires a spatial neighborhood, and the choice is a modeling decision with known trade-offs. The earlier point climatologies resolved it differently. Simpson and Lawrence (1971) used 80-km coastal segments. Keim et al. (2007), drawing on the storm-size literature (Dunn and Miller 1960; Simpson and Riehl 1981; Merrill 1984) and on the tendency for storm conditions to extend farther right of the track than left (Pielke and Pielke 1997), constructed an asymmetric, intensity-scaled swath: for hurricanes, hurricane conditions extend 80 km to the right of the track and 40 km to the left, with tropical-storm conditions a further 80 km right and 40 km left, and correspondingly wider bands for major hurricanes. NHC's HURISK-based products count storm centers within a symmetric 50 n mi circle, a radius NHC justifies as approximately the average maximum extent of hurricane-force winds (Blake et al. 2011).

We adopt the symmetric 50 n mi (92.6 km) center-proximity circle, fixed before any output was examined, for three reasons: it is the construct used by NHC's own return-period products, so our counts are comparable to the official ones; it is invariant to storm heading and requires no assumption about storm size; and it is transparent to reproduce. Its cost is that it ignores the right-left asymmetry and the size variation that Keim et al. modeled. We address that cost in two ways. Section 4.2 quantifies exactly what the two constructions do differently at 45 common sites, and Section 4.6 uses the modern per-storm analyzed wind radii, which did not exist for the earlier studies' records, to count envelope exposure directly for 2004-2025. Sensitivity of every core result to the radius (25, 50, 75, 100 n mi) is reported.

3.3 Coastal mesh and counting

We evaluate 33,916 candidate locations: 25,499 land-grid points at 0.1° spacing within 180 km of the coastline, 8,157 shoreline vertices for fine coastal geometry, and 260 explicitly sampled Florida Keys and Dry Tortugas points. This is the continuous generalization of the coastal-site design; it permits coastwide optimization without preselecting a city list. Reported coordinates identify the center of a high-scoring neighborhood, not a claim about one street corner.
Best-track position uncertainty at U.S. landfall is not constant over the window: the reanalysis literature places it near 60 n mi before 1944, near 20 n mi through the early aircraft-reconnaissance era, and near 12 n mi in the modern record (Landsea and Franklin 2013; Landsea et al. 2014; as compiled by Tolwinski-Ward 2015). Over the first third of our window it is therefore comparable to the neighborhood radius itself, and Tolwinski-Ward (2015) showed that treating landfall positions as exact enhances local maxima and narrows intervals most where rates are highest, a second selection effect at the optimized cell in addition to the winner's-curse premium. We therefore repeat the ranking analysis with landfall positions perturbed by era-appropriate errors (Section 4.3).

The candidate mesh over South Florida and Florida Bay

976 of the 33,916 evaluated locations fall in this frame

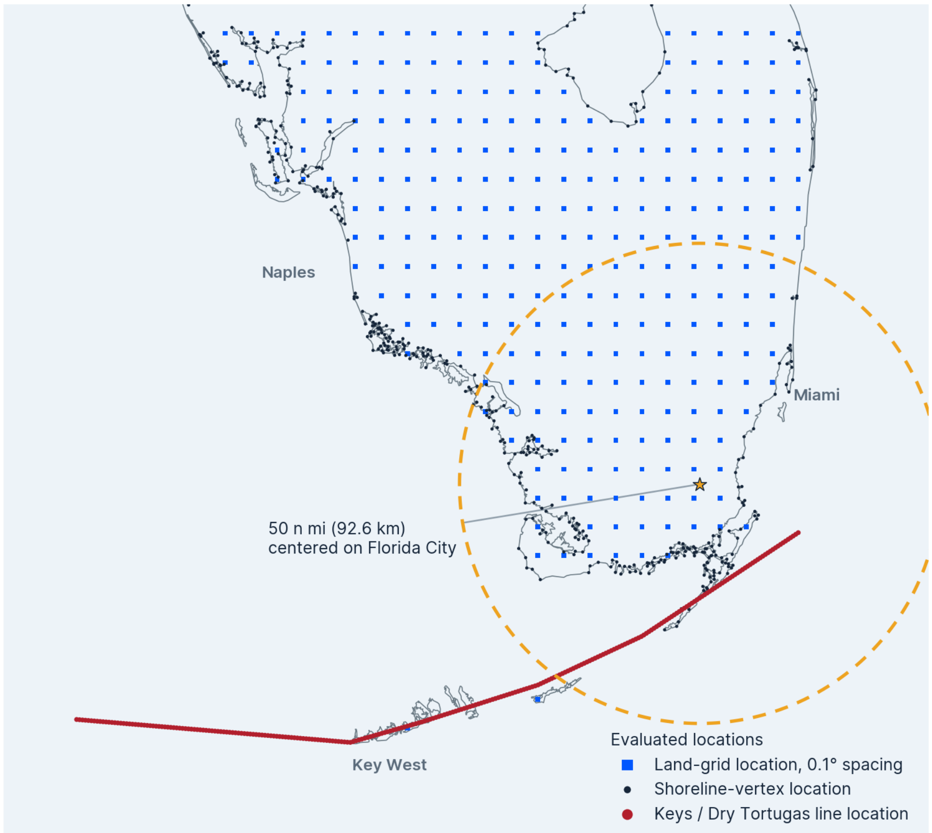

Figure 2. The candidate mesh over South Florida and Florida Bay: every evaluated location in the frame, by construction: 0.1° land-grid points (filled squares), shoreline vertices (small black dots), and the explicitly sampled Keys and Dry Tortugas line (red), with one 50 n mi neighborhood drawn to scale around Florida City. The shoreline vertices are evaluated exactly as the grid points are; they resolve the coastal edge, where the fields peak, at finer spacing than the grid. The land grid is confined to the high-resolution land mask, which is why the open water and wetlands of the Everglades and Florida Bay carry shoreline vertices rather than grid points.

Track positions are interpolated so that no segment exceeds about 18 km, preventing a fast-moving storm from crossing a candidate circle between six-hourly observations. Every metric counts a storm at most once at a given location, regardless of how long it lingers or how many nearby crossings it makes; a storm can legitimately count at two widely separated locations. For the wind-field metrics, the bearing from storm center to location selects the quadrant, and the location counts as covered when its distance is within the analyzed radius for that quadrant; missing radii are not imputed. For readable tables, a reported maximum within 200 km of a higher one is suppressed; this changes no counts, only which independent complexes are listed.

3.4 Statistics

For N events over T years we report the empirical rate N/T and its mean interval T/N; mean intervals are descriptive, not periodic. Intervals quoted with counts are exact Poisson bounds on the underlying rate. The Poisson assumption (variance equal to mean across seasons) is tested at each headline location by the variance-to-mean ratio, following Bove et al. (1998); where it is strained, a season-bootstrap interval that assumes no independence is reported alongside.

ENSO rate ratios carry exact conditional intervals (Clopper-Pearson on the binomial split of the total count), the construction Tartaglione et al. (2003) introduced for phase-conditioned landfall counts.

The coastwide search for a maximum is a fixed-window spatial scan statistic in the sense of Kulldorff (1997); the 200-km suppression reports non-overlapping secondary clusters. We do not apply the scan statistic's Monte Carlo test against a spatially uniform null, because uniformity is not a plausible null for hurricane occurrence along this coast; instead we characterize the *stability* of the ranking under resampling. Whole seasons are resampled with replacement, the full coastwide field is rebuilt on each of 2,000 replicates, and the maximum is located afresh each time; in a second experiment every landfall position is additionally perturbed by a normal draw with the era-dependent uncertainty above, alone and jointly with season resampling. We report how often each region holds the maximum, the distribution of the leading count, and the resampling interval of the margin between leading regions. Season resampling treats seasons as exchangeable, which is optimistic if there is multidecadal structure; the lag-1 autocorrelation of annual continental U.S. landfall counts is 0.11 (Klotzbach et al. 2018), so the approximation is reasonable for this series. These procedures answer the concern that a maximum picked out of many candidates is selected because it is large (Gelman and Price 1999; Wilks 2016) by measuring how often the selection would repeat.

3.5 Pre-commitment

The following were fixed before any field was computed and were not revised: the 50 n mi radius; ≥64 kt and ≥96 kt as the hurricane and major-hurricane thresholds at the qualifying position; the 1900-2025 comparison window; one count per storm per location; no imputation of missing wind radii; and the 200-km suppression rule for listing. Sensitivity to radius and to window is reported rather than tuned.

4. Results

4.1 The three focal points, 1900-2025

Under all three occurrence definitions the field concentrates in the same three regions the earlier climatologies identified: the south Florida peninsula and Keys, the Outer Banks of North Carolina, and the north-central Gulf Coast. Which of the three leads depends on the definition.

Coastline crossings (L50). The largest direct-landfall neighborhood is in south Florida. The optimized 50 n mi neighborhood in the Florida Bay/Everglades sector contains 26 hurricane-strength crossings in 1900-2025, a mean interval of 4.85 yr (95% CI 3.3-7.4). Southeast Louisiana follows with 20 and southeastern North Carolina with 18.

Rank	Region	Storms	Mean interval (yr)	95% CI (yr)
1	South Florida / Florida Bay	26	4.85	3.3-7.4
2	SE Louisiana / Terrebonne-Lafourche	20	6.30	4.1-10.3
3	SE North Carolina / Cape Fear	18	7.00	4.4-11.8
4	Mississippi-Alabama coast	17	7.41	4.6-12.7
5	Upper Texas / Galveston sector	17	7.41	4.6-12.7
6	Western Florida Panhandle	15	8.40	5.1-15.0

Rank	Region	Storms	Mean interval (yr)	95% CI (yr)
7	Charleston / South Carolina	14	9.00	5.4-16.5
8	South Texas / Padre Island	12	10.50	6.0-20.3
9	Central Texas / Matagorda	11	11.45	6.4-22.9
10	Central Florida Atlantic coast	10	12.60	6.9-26.3
11	Long Island, New York	8	15.75	8.0-36.5
12	Outer Banks, North Carolina	8	15.75	8.0-36.5

Direct hurricane landfall hotspots shift after correcting the historical exposure window

The raw 1851 archive favors southeast Louisiana; the common 1900 start moves the maximum to South Florida.

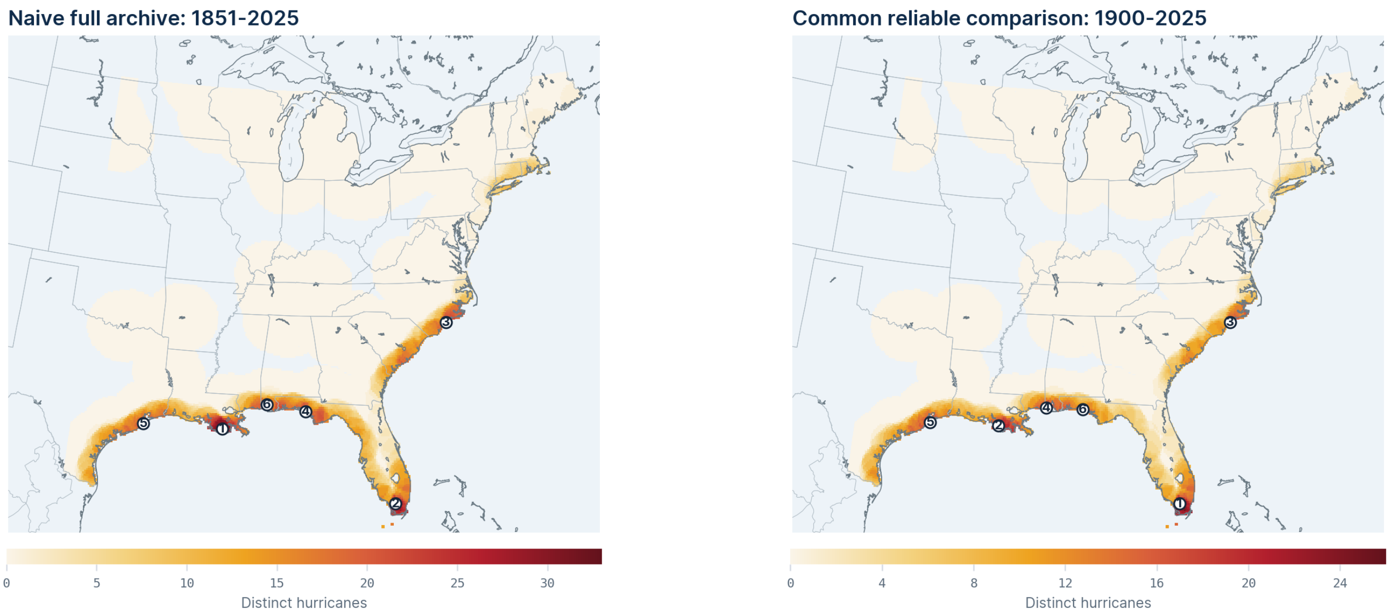

Figure 3. L50 fields for the full archive and for the common reliable window.

Among inhabited places, Florida City and Homestead each record 23 nearby crossings (5.48 yr; 95% CI 3.7-8.6), the highest of any community tested. The optimized cell counts 26; the difference of about 13% is the selection premium that any post hoc maximum carries, and named-place values are the ones to quote for a specific town.

Place	L50 1900-2025	Mean interval (yr)	95% CI (yr)	El Niño	La Niña	Neutral
Florida City, FL	23	5.48	3.7-8.6	2	2	5
Homestead, FL	23	5.48	3.7-8.6	2	2	5
Houma, LA	19	6.63	4.2-11.0	2	4	7
Miami, FL	17	7.41	4.6-12.7	2	1	4
Pensacola, FL	16	7.88	4.8-13.8	2	4	3
Mobile, AL	15	8.40	5.1-15.0	2	3	2

Place	L50 1900-2025	Mean interval (yr)	95% CI (yr)	El Niño	La Niña	Neutral
Gulf Shores, AL	15	8.40	5.1-15.0	2	3	3
Galveston, TX	15	8.40	5.1-15.0	1	2	4
Charleston, SC	14	9.00	5.4-16.5	2	2	5
Port O'Connor, TX	13	9.69	5.7-18.2	0	3	2

Center passages (H50). Broadening the event to any hurricane center within 50 n mi moves the maximum to the Outer Banks: 35 storms at Cape Hatteras (3.60 yr; 95% CI 2.7-5.2), with south Florida at 29 and southeast Louisiana at 25. The named Cape Hatteras point counts 32, a selection premium of about 9%. NHC's tabulated return periods point the same way: among the 66 communities listed in Blake et al. (2011), Cape Hatteras has the shortest hurricane return period, five years, ahead of Miami at six.

Rank	Region	Storms	Mean interval (yr)	95% CI (yr)
1	Cape Hatteras / Outer Banks	35	3.60	2.6-5.2
2	South Florida / Florida Bay	29	4.34	3.0-6.5
3	SE Louisiana / Terrebonne	25	5.04	3.4-7.8
4	Upper Texas / Galveston sector	23	5.48	3.7-8.6
5	South Carolina coast	23	5.48	3.7-8.6
6	Central Florida	22	5.73	3.8-9.1
7	Mississippi-Alabama-western Florida	21	6.00	3.9-9.7
8	Florida Big Bend	17	7.41	4.6-12.7
9	South Texas	16	7.88	4.8-13.8
10	Acadiana / SW Louisiana	12	10.50	6.0-20.3
11	Delmarva / Virginia coast	12	10.50	6.0-20.3
12	Northeast Florida	9	14.00	7.4-30.6

Frequency and intensity have different national maxima

Cape Hatteras/Outer Banks leads nearby hurricane-center frequency; South Florida leads nearby major-hurricane frequency.

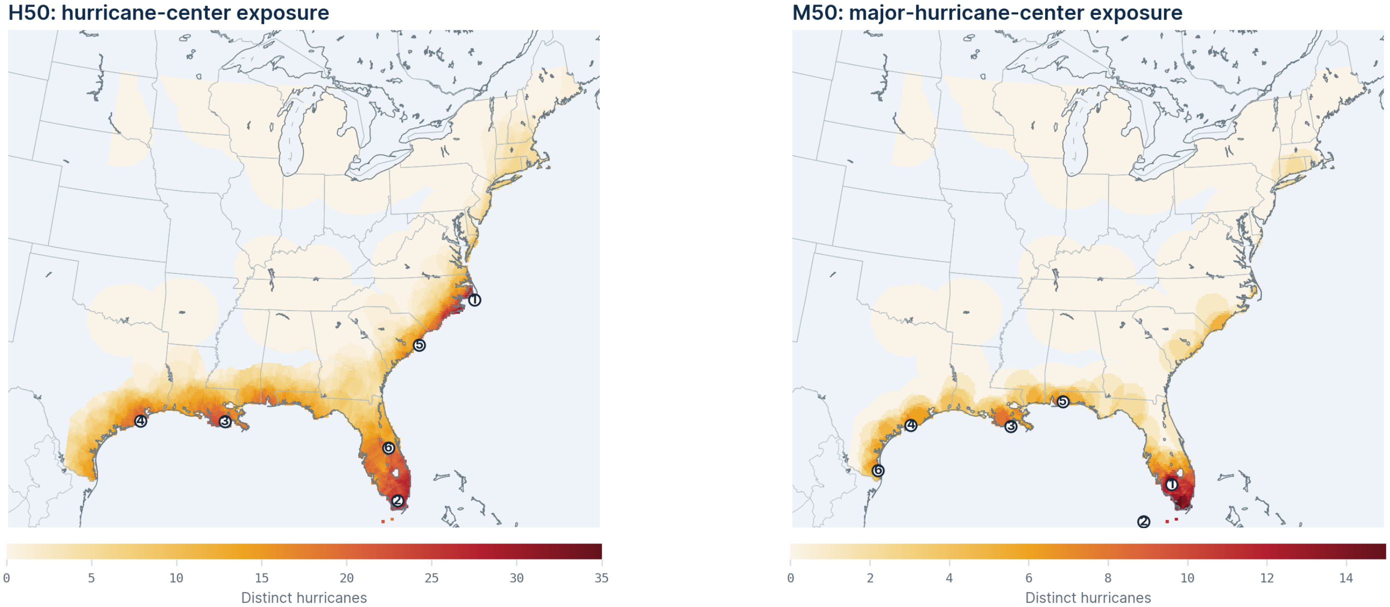

Figure 4. H50 and M50 fields, 1900-2025.

The Outer Banks lead the center-passage metric for a geometric reason: they protrude into the western Atlantic beside the recurvature corridor, so storms that make landfall, graze the barrier islands, remain offshore, or re-emerge after a mainland crossing all pass through the local circle. South Florida and southeast Louisiana earn most of their exposure from crossings; the Outer Banks earn an unusually large share from offshore passage. Eastern North Carolina remains the H50 maximum at 25, 50, 75, and 100 n mi.

Major-hurricane passages (M50). Conditioning on intensity returns the maximum to south Florida: 15 major-hurricane passages in the optimized south/southwest Florida neighborhood (8.40 yr; 95% CI 5.1-15.0), with the Dry Tortugas and Keys at 12.

Rank	Region	Storms	Mean interval (yr)	95% CI (yr)
1	South / southwest Florida	15	8.40	5.1-15.0
2	Dry Tortugas / Florida Keys	12	10.50	6.0-20.3
3	SE Louisiana / lower delta	9	14.00	7.4-30.6
4	Central Texas coast	9	14.00	7.4-30.6
5	Western Florida / Alabama	8	15.75	8.0-36.5
6	South Texas	7	18.00	8.7-44.8
7	South Carolina coast	6	21.00	9.6-57.2
8	Outer Banks, North Carolina	5	25.20	10.8-77.6

Radius sensitivity. South Florida remains the L50 maximum at 25, 50, 75, and 100 n mi, though the maximizing point moves around the peninsula and bay system as the radius grows.

Radius (nmi)	Direct landfalls L(r)	L per 100 yr	Center passages H(r)	H per 100 yr
25	12	9.5	20	15.9
50	26	20.6	35	27.8
75	37	29.4	49	38.9
100	45	35.7	57	45.2

Radius is an estimand, not a neutral formatting choice

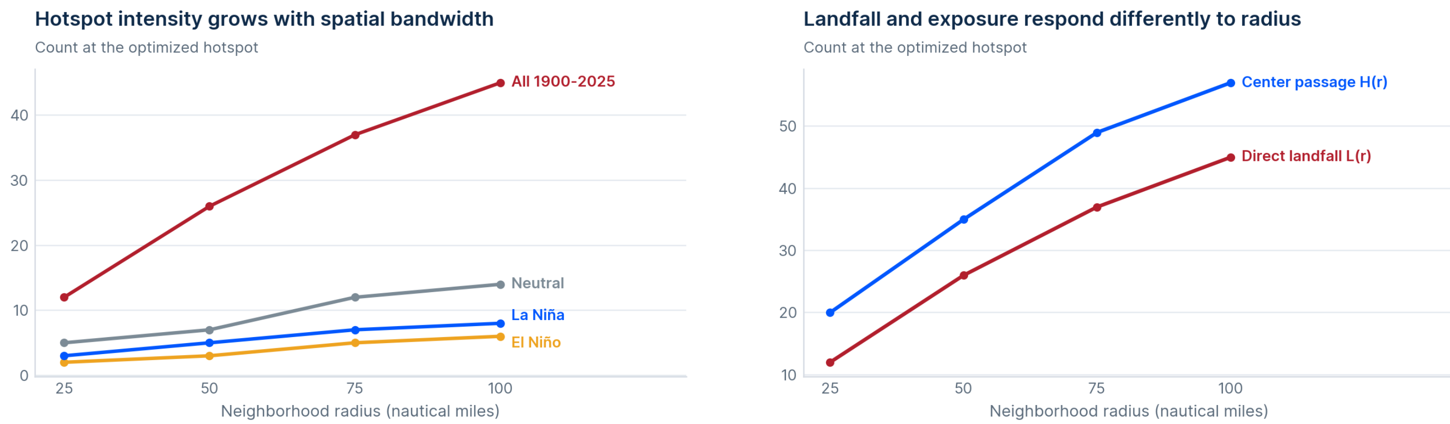

Figure 5. Optimized-hotspot counts as the neighborhood radius varies.

Record length. If every year from 1851 is treated as equally observed, southeast Louisiana leads the crossing count (33 to south Florida's 30). The common window removes the poorly observed nineteenth-century south Florida years, which the raw archive treats as known zeroes, and the maximum moves to south Florida. In the 1950-2025 record alone, southeast Louisiana leads with 14, southeastern North Carolina has 13, and south Florida 12: recent Louisiana clustering is real, and the long-record south Florida result is not invariant to period.

4.2 Comparison with the earlier climatologies

To place these results against Keim et al. (2007) without confounding method with record length, we computed our three intensity tiers (≥34, ≥64, ≥96 kt at the qualifying position) at their 45 site coordinates over their window, 1901-2005, and compared with the return periods they report.

Intensity tier	Sites	Median ratio, this study / KMS	Interquartile range	Rank correlation (Spearman)	KMS value within our 95% interval
TS+	45	0.90	0.80-1.01	0.84	96%
Hurricane	44	0.70	0.50-0.82	0.88	80%
Major	25	0.60	0.50-0.71	0.86	84%

The two constructions agree on where and disagree on how often, by a factor the geometry predicts. Rank correlation is 0.84-0.88 at every tier, and seven of the ten sites with the shortest hurricane intervals are shared (Cape Hatteras, Miami Beach, Palm Beach, Key Largo, Key West, Marco Island, Dauphin Island); the three each study adds belong to the same three focal points. Our intervals are systematically shorter, by a median factor of 0.90 for tropical-storm-and-stronger, 0.70 for hurricanes, and 0.60 for majors. Both features follow from the two geometries. Keim et al.'s swath is asymmetric and intensity-scaled: hurricane conditions extend 80 km right and 40 km left of track for a Category 1-2 storm, and for a major hurricane the major-condition band is 80 km right and 40 km left with weaker-hurricane conditions a further 80 km right and 40 km left. Our circle reaches 92.6 km in every direction and assigns intensity from the center's wind at the qualifying position. Storms passing between 40 and 92.6 km to the left of a site therefore count for us and not for them at every tier; and their strike intensity is assigned by which band of the swath the site falls in, so a major hurricane whose center passes 60 km to the left of a site is a "major" for us and a "hurricane" for them, and one passing 100 km to the right is a hurricane for them and nothing for us. The net effect is a shorter interval for us at every tier, growing with intensity because the band assignment demotes more of their events at higher tiers, which is the gradient observed.

Site	Hurricane, KMS 1901-2005	This study, 1901-2005	This study, 1900-2025	Major, KMS	This study, 1901-2005	This study, 1900-2025
Cape Hatteras, NC	5	3.5	3.7	35	21.0	25.2
Atlantic Beach, NC	8	4.0	4.1	52	52.5	63.0
Miami Beach, FL	5	3.9	4.7	18	8.8	10.5
Key Largo, FL	4	4.2	5.0	13	8.1	9.7
Key West, FL	5	4.8	5.5	15	9.5	10.5
Palm Beach, FL	5	4.2	4.7	18	13.1	14.0
Marco Island, FL	7	5.2	6.0	15	9.5	10.5
Pensacola Beach, FL	6	6.2	7.0	21	15.0	18.0
Boothville, LA	7	7.5	7.0	26	21.0	21.0
Galveston, TX	8	6.6	6.6	26	21.0	21.0
St. Petersburg, FL	26	6.2	6.6	52	26.2	25.2
Cedar Key, FL	35	13.1	12.6	105	52.5	42.0

The site-level exceptions confirm the mechanism. At Cedar Key (their 35 yr, our 13.1), which Keim et al. name as a sheltered coastline, and at St. Petersburg (26 vs 6.2), coastline orientation and parallel offshore tracks make the left-right asymmetry decisive; their swath registers the sheltering and our symmetric circle does not. Where tracks cross the coast roughly perpendicularly, at Boothville (7 vs 7.5) and Pensacola Beach (6 vs 6.2), the two methods agree to within a year. Extending the window from 2005 to 2025 shortens most intervals modestly, most visibly on the Gulf and in Florida.

The comparison with NHC is of a different kind. NHC's Table 12 and its return-period maps count hurricanes passing within 50 n mi of a location (Blake et al. 2011), the same event as our H50; the difference is that NHC's values are HURISK model estimates (Neumann 1987), fitted on the record from 1886, while ours are empirical counts. Our H50 intervals run about 0.74 of NHC's across the eleven listed communities, and the ratio is essentially the same whether we count on 1851-2010, on HURISK's own 1886-2010, on 1900-2010, or on 1900-2025 (medians 0.72-0.75), so the offset is not a window or record-length effect but a model-versus-count one: the smoothed model returns longer intervals than the raw count at these points, while preserving their order. We report both and do not adjust one to the other. Readers who need modeled return periods should use NHC's products; ours are the empirical counts on the current record.

The often-quoted description of Monroe County as the most hurricane-prone county in the United States, with a roughly four-year return period, originates in Elsner and Kara's (1997) county-level climatology for 1900-1996, which counts direct and indirect strikes anywhere in a county; NHC's 50 n mi return period for the single point of Key West is eight years, and the two figures answer different questions on different geographic supports. The county-to-point ratio, 4 to 8 for Monroe and 5 to 6 for Miami-Dade in those sources, is reproduced by our own county-integrated and single-point H50 counts over 1900-2025 (0.56 for Monroe County against Key West, 0.78 for Miami-Dade against Miami) and by Jagger et al.'s (2001) county-to-point factor of 0.48 for a Keys-scale county; the ordering is the same in every pair, and Monroe's lower ratio reflects a county that spans 275 km of archipelago, several times the circle's diameter.

Location	Empirical H50 (yr)	NHC hurricane (yr)	Empirical M50 (yr)	NHC major (yr)
Cape Hatteras, NC	4.0	5.0	17.8	16.0
Morehead City, NC	4.3	6.0	40.0	18.0
Wilmington, NC	5.7	7.0	26.7	18.0
Miami, FL	4.7	6.0	11.4	14.0
Fort Lauderdale, FL	4.7	7.0	11.4	16.0
Key West, FL	5.2	8.0	14.5	18.0
Charleston, SC	6.7	8.0	40.0	22.0
Houma, LA	5.5	8.0	16.0	20.0
Galveston, TX	6.4	9.0	26.7	25.0
Gulf Shores, AL	6.7	9.0	16.0	25.0
New Orleans, LA	6.7	10.0	20.0	23.0

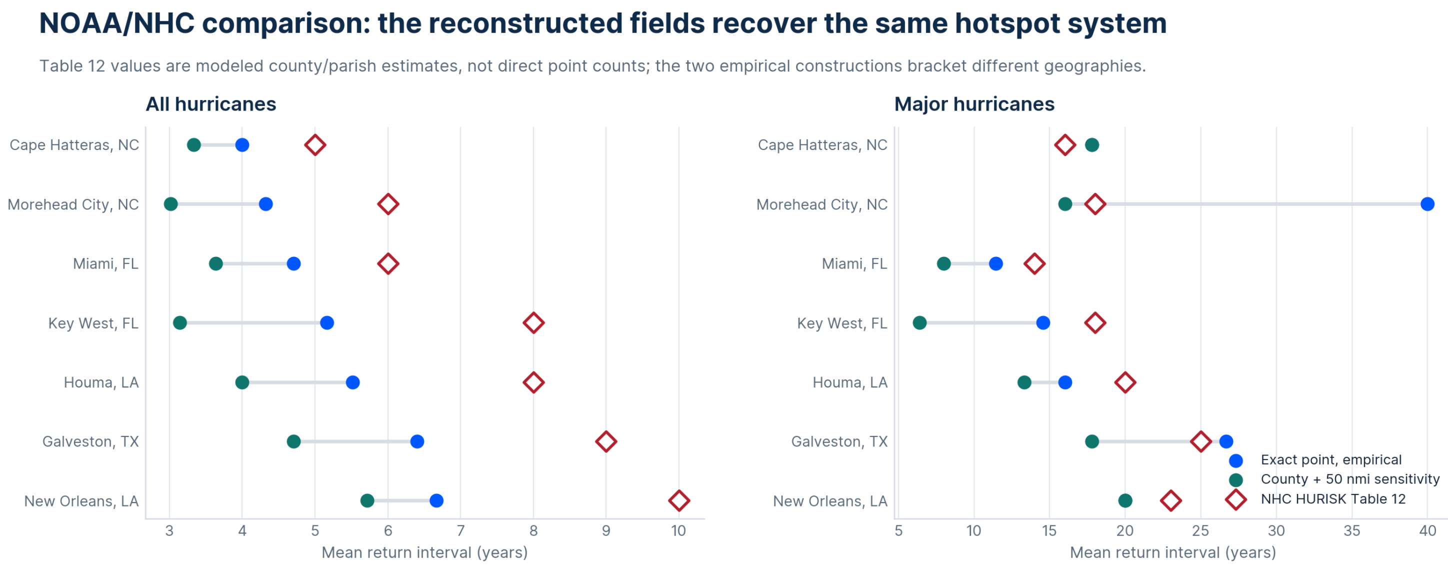

Figure 6. Exact-point empirical intervals against NHC modeled county values.

4.3 How sure is the ranking?

Metric	Leading complex	Storms	Leads in season resamples	Runner-up	Runner-up share
L50	South Florida / Florida Bay	26	69%	SE Louisiana / Terrebonne-Lafourche	13%
H50	Cape Hatteras / Outer Banks	35	63%	South Florida / Florida Bay	28%
M50	South / southwest Florida	15	64%	Dry Tortugas / Florida Keys	32%

Under season resampling alone, south Florida holds the L50 maximum in 69% of replicates; southeast Louisiana takes it in 13% and southeastern North Carolina in 6%; the observed margin of six storms over Louisiana has a 95% resampling interval of −6 to +17. Cape Hatteras holds the H50 maximum in 63% of replicates with south Florida at 28% (margin interval −11 to +18). The south/southwest Florida and Dry Tortugas neighborhoods together hold the M50 maximum in 96% of replicates, so the location of the major-hurricane pole is far more secure than the ordering within it.

Perturbing landfall positions by their era-dependent uncertainty changes the crossing result materially. With positions perturbed and all seasons kept, south Florida still holds the L50 maximum in 71% of replicates, but the count at the optimized cell falls from 26 to a median of 19 (95% range 15-23) and its margin over southeast Louisiana shrinks to a median of one storm; the 60 n mi pre-1944 uncertainty smears the compact Florida Bay cluster far more than the Louisiana coast, exactly the effect Tolwinski-Ward (2015) describes. Perturbing positions and resampling seasons jointly, south Florida holds the maximum in 45% of replicates and southeast Louisiana in 28%, with the margin interval −9 to +12 and south Florida ahead in 53%. The crossing-metric ranking is therefore closer to even than the season bootstrap alone suggests, and the 26-storm count at the optimized cell should be read as the count on the recorded positions, not as a precise estimate.

Resampling scheme	South Florida holds L50 maximum	Southeast Louisiana	Margin, 95% interval	Count at optimized cell, median (95%)
Seasons only	69%	13%	−6 to +17	26 (recorded)
Positions only	71%	27%	-4 to +6	19 (15-23)
Seasons and positions	45%	28%	-9 to +12	20 (13-31)

The honest statement is that south Florida is the most probable crossing maximum, with southeast Louisiana a nearly equal alternative once position uncertainty is admitted; the most probable and, under position perturbation, still clearly leading major-hurricane maximum; and that the Outer Banks are the most probable center-passage maximum. What raises confidence in the south Florida result beyond any single count is convergence: it is the L50 maximum at all four radii on the recorded positions, it is simultaneously the M50 maximum, and it is the maximum on the common window that the earlier climatologies also identified. No other region has that combination.

4.4 Repeated-hit seasons

A storm counts once per location, but a season can deliver more than one storm, and the difference between storm counts and exposed-year counts is not uniform along the coast.

Place	H50 storms	Exposed years	Mean H50 interval (yr)	M50 storms
Cape Hatteras, NC	32	31	3.94	5
Morehead City, NC	31	28	4.06	2
Miami, FL	28	22	4.50	13
Florida City, FL	28	21	4.50	14
Homestead, FL	27	21	4.67	13
West Palm Beach, FL	27	19	4.67	9
Key West, FL	23	20	5.48	12
Houma, LA	21	21	6.00	8
Wilmington, NC	20	19	6.30	5
Charleston, SC	19	16	6.63	4

Repeated-hit seasons are unusually important in South Florida

Nearby hurricanes (H50) and seasons with at least one, 1900-2025

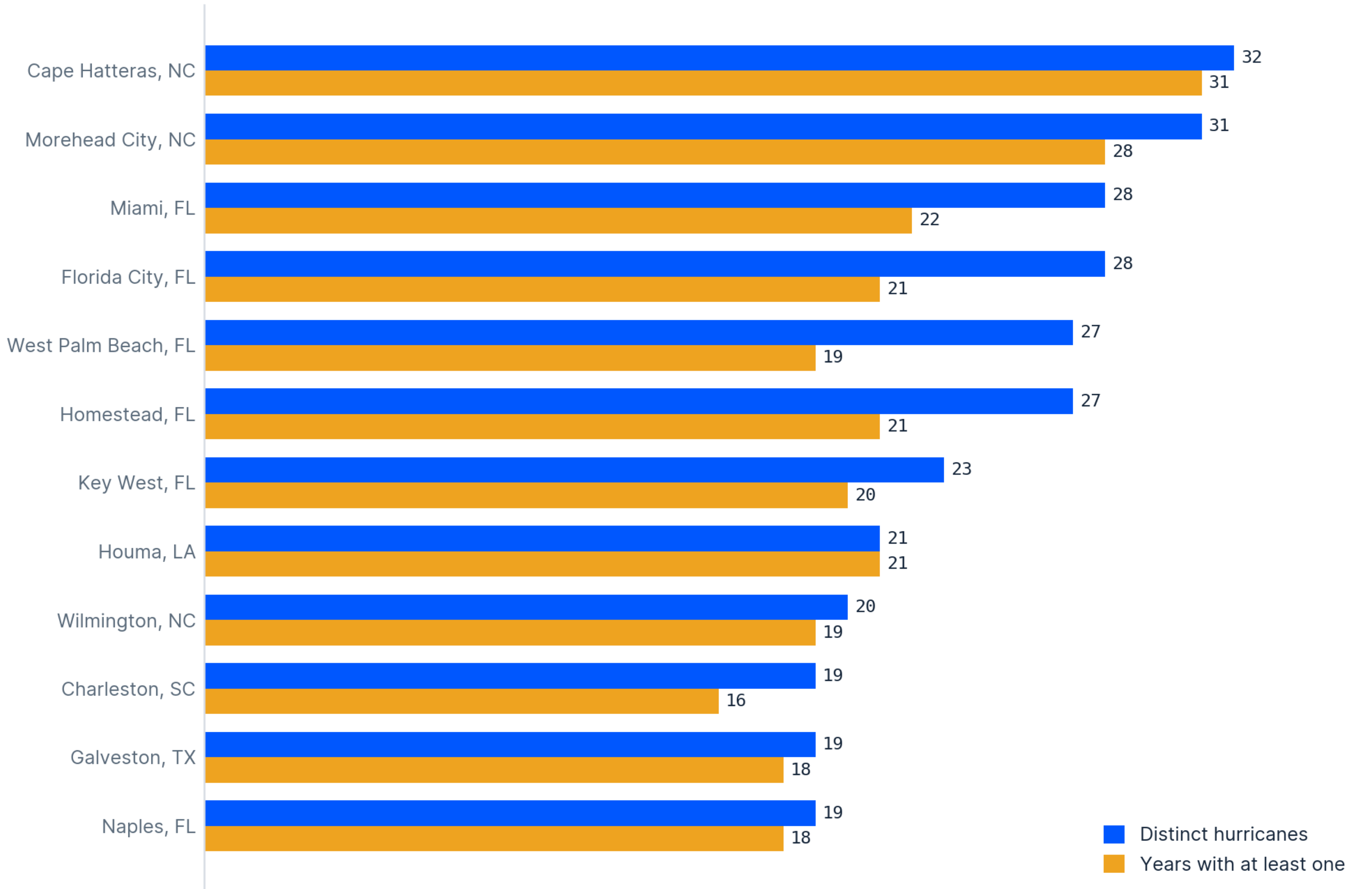

Figure 7. Storm counts against exposed-year counts for the leading places.

Cape Hatteras records 32 nearby hurricanes in 31 distinct years: almost never two in a season. South Florida's exposure is clustered: Miami's 28 storms arrive in 22 distinct years, Florida City's 28 in 21. The same property appears in the seasonal count statistics. At south Florida the annual counts are overdispersed relative to Poisson (variance-to-mean ratio 1.19, $p \approx 0.07$ for the L50 cell; 1.26, $p \approx 0.03$ for the H50 cell), the Florida clustering that Jagger and Elsner (2012) report, while the Louisiana and North Carolina cells pass. Where the Poisson assumption strains, we report season-bootstrap intervals alongside: for the south Florida landfall cell, 3.4-7.9 yr against the Poisson 3.3-7.4; the difference is about a tenth of the interval width and no conclusion depends on it.

Elsner and Kara (1997) reported the same property for the state of Florida from the 1851-1996 record: 91 landfalls in 63 distinct years, with a 41% probability of a second landfall in a year that already has one. On the same window, counting strict hurricane-status crossings inside the Florida state polygon, our catalogue gives 85 to 90 storms in 60 to 62 distinct years and a 37 to 40% conditional probability, the range reflecting how far offshore a landfall coordinate is allowed to sit; the small shortfall against their count follows from their broader event, which includes indirect strikes. The practical significance is greater than the statistical one. A region whose hurricanes arrive in clusters faces a distinct planning problem: recovery from one storm can be interrupted by the next within the same season, and the effective demand on evacuation, shelter, insurance, and repair capacity is set by the multi-storm season, not by the mean interval. South Florida's mean interval understates that demand in a way the Outer Banks' does not.

4.5 ENSO stratification: Bove et al. (1998) revisited

Bove et al. (1998) classified 1900-1997 U.S. landfalling hurricanes by ENSO phase, tested each phase for Poisson dispersion, and used a bootstrap for confidence limits, finding mean rates of 1.04, 1.61, and 2.23 hurricanes per season in El Niño, neutral, and La Niña years and probabilities of two or more landfalls of 28%, 48%, and 66%. We repeat that design on the strict landfall catalogue for 1950-2025 with the RONI classification.

Phase	Seasons	Hurricanes	Mean / season	Seasons with ≥1	Seasons with ≥2
El Niño	20	20	1.00	65%	15%
Neutral	36	56	1.56	75%	44%
La Niña	20	40	2.00	85%	55%

Comparison	Rate ratio	95% CI
La Niña vs El Niño	2.00	1.14-3.61
Neutral vs El Niño	1.56	0.92-2.74
La Niña vs Neutral	1.29	0.83-1.96

Phase	Bove et al. 1900-1997, mean per season	This study 1950-2025, mean per season	Bove et al., P(≥2 landfalls)	This study, P(≥2 landfalls)
El Niño	1.04	1.00	28%	15%
Neutral	1.61	1.56	48%	44%
La Niña	2.23	2.00	66%	55%

La Niña roughly doubles the strict U.S. hurricane-landfall rate relative to El Niño

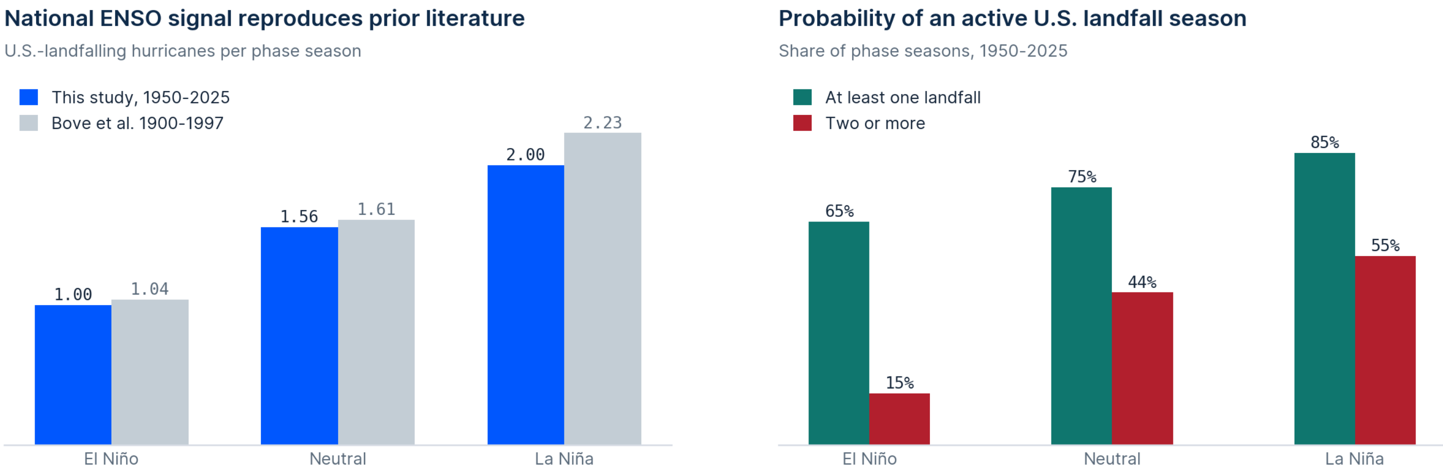

Figure 8. Phase landfall rates and active-season probabilities, 1950-2025.

The phase structure reproduces. La Niña seasons show twice the strict landfall rate of El Niño seasons (2.00; exact 95% CI 1.14-3.61); of the three pairwise comparisons only La Niña versus El Niño excludes a ratio of one. Our probabilities of an active season run below Bove et al.'s because their event, a storm delivering hurricane-force winds to the coast, is broader than a strict center crossing; the ordering and the approximate doubling are the same. The agreement validates the phase partition, since two different indices assign substantively the same seasons to the same phases over the overlapping years; it does not validate the landfall catalogue, which is checked against NHC's products above. The effect is one of frequency, not extremity: published extreme-value analysis finds the rarest landfalling wind speeds if anything higher in El Niño years (Jagger and Elsner 2006).

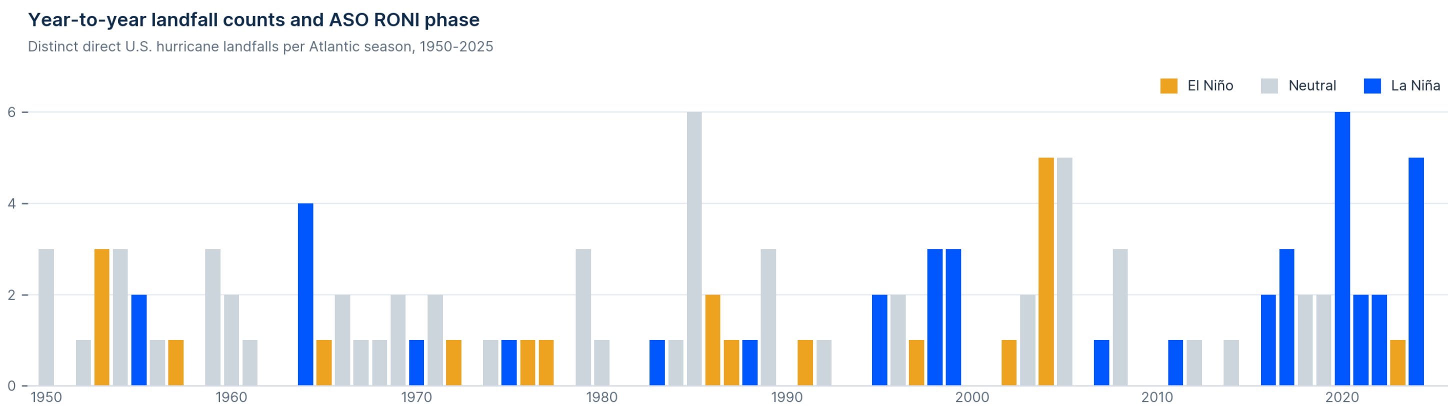

Figure 9. Annual strict U.S. hurricane-landfall counts by ASO RONI phase.

The national rate effect is far more robust than any phase-conditioned destination. El Niño's strongest local concentration is three storms in twenty seasons; La Niña's sharpest is five, in southeastern North Carolina, consistent with Klotzbach's (2011) state-level finding that warm-cold probability differences are largest along the East Coast and in particular North Carolina. With counts this small we treat the maps as retrospective conditional climatology; answering the phase-conditioned "where" with confidence has required stochastic track models (Hall and Yonekura 2013).

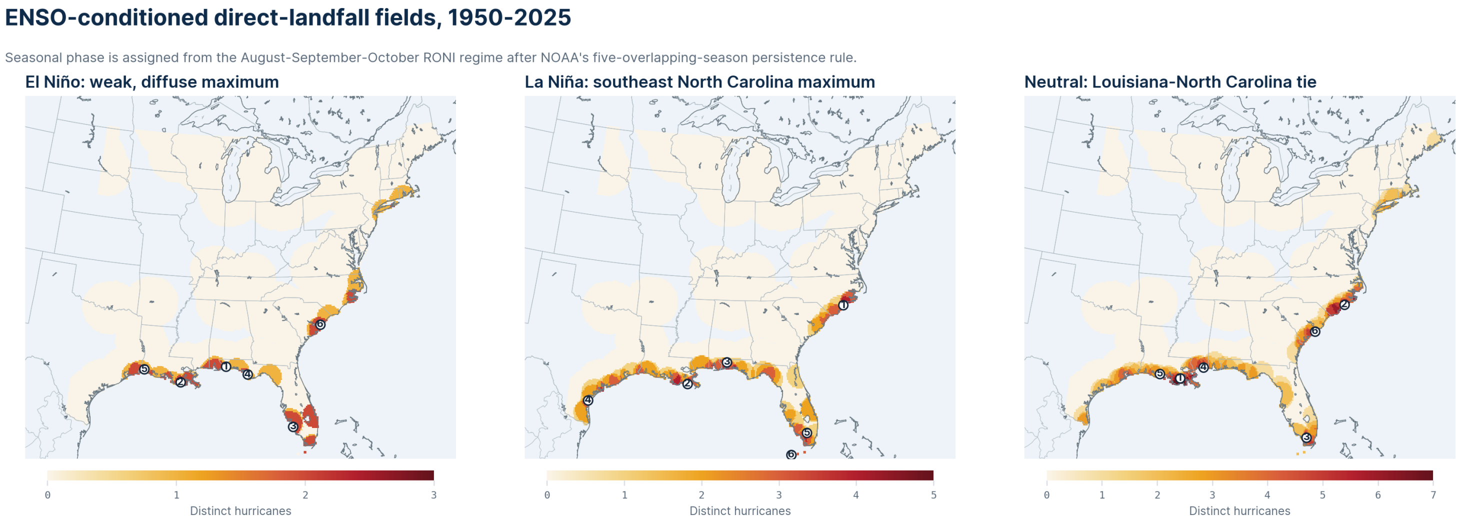

Figure 10. Where each phase has put its landfalls, 1950-2025.

4.6 Modern wind-field envelopes, 2004-2025

A fixed radius cannot represent storm size, which the storm-size literature shows to be highly variable and only weakly related to intensity (Merrill 1984; Chavas and Emanuel 2010; Chavas et al. 2016). Since 2004 the best-track record includes analyzed quadrant wind radii, so for the modern era we can count locations inside the analyzed wind field directly. Two cautions govern the reading. The record is short: 22 seasons support a cross-check, not a century-scale interval, and the counts are descriptive. And the radii are analyzed maximum extents by quadrant, with published relative uncertainty of roughly 25-30% even at landfall, against about 7% for position (Landsea and Franklin 2013). Being inside the analyzed 64-kt envelope is a statement about the analyzed maximum extent in that quadrant, not a measurement that a location experienced hurricane-force winds; because a quadrant's radius is a maximum applied to the whole quadrant, the counts are best read as an upper bound on the sector geometry, even though the radii themselves are if anything biased slightly low against independent surface-wind analyses (Combot et al. 2020). Missing radii are not imputed, which biases the counts downward.

Counting locations inside the 64-kt envelope, no unique maximum emerges: the Dry Tortugas and Keys, eastern North Carolina near Morehead City, the lower Mississippi Delta, and central Florida tie at six storms each. Because a quadrant's analyzed radius is a maximum rather than a representative extent within that quadrant, we recomputed with every radius scaled to 85%, the ratio the county-exposure literature applies to these same radii for that reason (Knaff et al. 2016; Anderson et al. 2020); three of the four regions remain at six and central Florida drops to five, so the multi-modal picture is not an artifact of taking the envelope at face value. Twenty-two seasons cannot separate a four-way tie at six, and we present it as the resolution the record permits rather than as a finding of parity.

Region	Storms	Contributing hurricanes
Dry Tortugas / Florida Keys	6	2004 Charley; 2005 Dennis; 2005 Katrina; 2005 Rita; 2005 Wilma; 2022 Ian
Eastern North Carolina / Morehead	6	2005 Ophelia; 2011 Irene; 2014 Arthur; 2016 Matthew; 2018 Florence; 2019 Dorian
Lower Mississippi Delta	6	2004 Ivan; 2005 Katrina; 2008 Gustav; 2012 Isaac; 2017 Nate; 2021 Ida

Region	Storms	Contributing hurricanes
Central Florida	6	2004 Charley; 2004 Frances; 2004 Jeanne; 2017 Irma; 2022 Ian; 2024 Milton
SW Louisiana / upper Texas	4	2005 Rita; 2008 Ike; 2020 Laura; 2020 Delta
Florida Big Bend	4	2016 Hermine; 2023 Idalia; 2024 Debby; 2024 Helene
Grand Strand / South Carolina	4	2016 Matthew; 2018 Florence; 2019 Dorian; 2020 Isaias
Acadiana / central Louisiana	3	2008 Gustav; 2019 Barry; 2024 Francine
Southwest Florida / Everglades	3	2005 Katrina; 2005 Wilma; 2017 Irma
Upper Texas coast	3	2008 Ike; 2021 Nicholas; 2024 Beryl

Recent wind-radius data produce a multi-pole exposure field

R64 has a four-way maximum of six storms; R34 emphasizes the Keys, South Carolina, southeast Louisiana, and Florida.

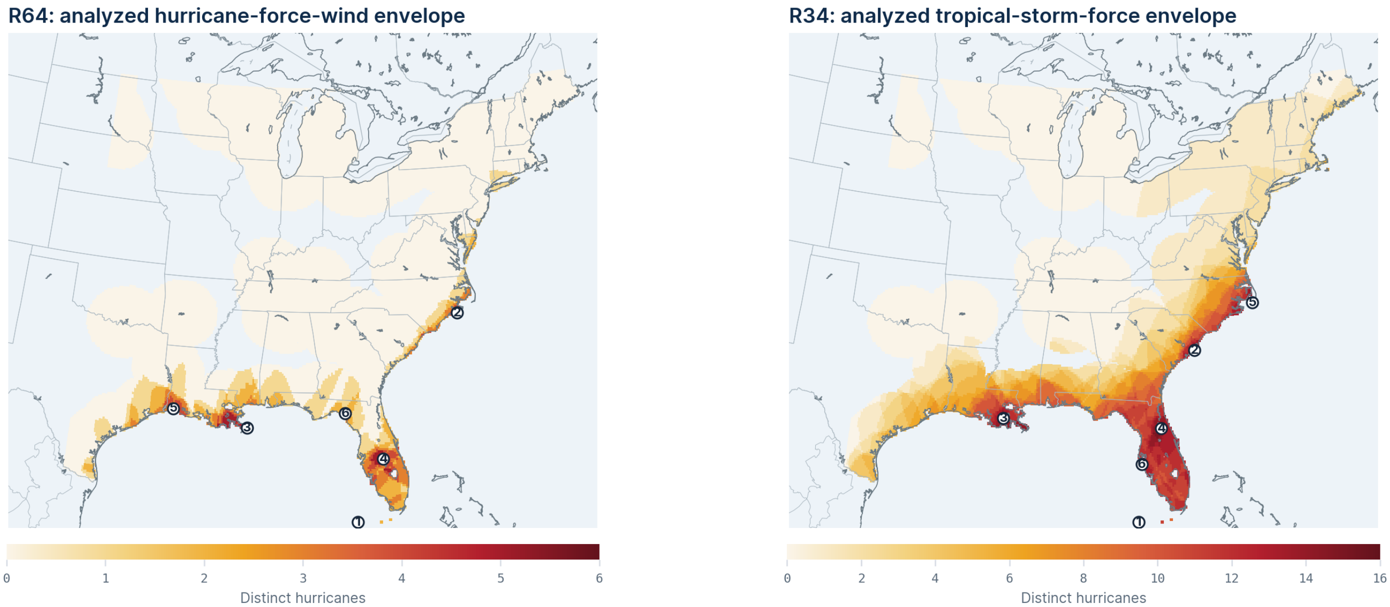

Figure 11. R64 and R34 envelope exposure, 2004-2025.

Southeast Louisiana rises relative to many regions when actual wind-field size is used, and central Florida's interior maximum, produced by storms crossing from both the Atlantic and Gulf sides, shows that a location need not be coastal to be exposed. The 34-kt envelope, counted while the storm is a hurricane, saturates faster and emphasizes breadth of the circulation rather than its core.

Rank	Region	Storms	Mean interval (yr)	95% CI (yr)
1	Dry Tortugas / Florida Keys	16	1.38	0.8-2.4
2	South Carolina coast	16	1.38	0.8-2.4
3	SE Louisiana / Terrebonne	15	1.47	0.9-2.6
4	North-central Florida Atlantic	15	1.47	0.9-2.6

Rank	Region	Storms	Mean interval (yr)	95% CI (yr)
5	Cape Hatteras / Outer Banks	14	1.57	0.9-2.9
6	West-central Florida / Tampa	14	1.57	0.9-2.9
7	Southeast Florida	13	1.69	1.0-3.2
8	Florida Big Bend	12	1.83	1.0-3.5

5. Discussion

The updated climatology recovers the three focal points that Simpson and Lawrence (1971), Elsner and Kara (1999), and Keim et al. (2007) identified, under a different event construction and on the current reanalyzed record, with rank agreement above 0.84 at every intensity tier against the most recent of them. That agreement across constructions is the strongest single check on the computation. Keim et al. (2007) already showed that the leader depends on the tier: the Outer Banks lead their tropical-storm-and-stronger map, tie south Florida for hurricanes, and lose to south Florida by a factor of two for majors, and their hazard index separates Cape Hatteras (most strikes) from Key Largo (most majors) in the same way. We recover that structure under a different event construction, on a continuous mesh with no preselected site list, on the current reanalyzed record. What the earlier studies did not do, and this analysis adds, is quantify how sure each ranking is.

The three-pole structure of continental U.S. hurricane exposure

No single metric exhausts "exposure." The leading regions specialize in different dimensions.

Outer Banks / Cape Hatteras
Frequency maximum

H50 national maximum	35
Cape Hatteras storms	32
Exposed years, 1900-2025	31

Offshore recurvature adds exposure

South Florida
Intensity maximum

M50 national maximum	15
L50 common-period maximum	26
Florida City M50 storms	14

Multi-hurricane seasons matter

Southeast Louisiana
Large wind fields, recent maximum

L50 raw archive maximum	33
H50 hotspot count	25
R64 lower-delta maximum	6

Large mature Gulf hurricanes

Synthesis: eastern North Carolina is exposed most often, South Florida receives the most close major-hurricane passages, and southeast Louisiana is especially prominent when actual recent wind-field size is used.

Figure 12. The three regimes and their leading metrics.

The three regions are best understood as three exposure regimes, a reading prefigured by Keim et al.'s hazard index and by the Gulf and East Coast landfall clusters of Elsner et al. (2000). The Outer Banks are the frequency regime: many hurricanes pass nearby, including offshore and recurving storms, but comparatively few are major at closest approach. South Florida is the crossing and intensity regime: several approach corridors converge on one small neighborhood, producing the most crossings, the most close major-hurricane passages, and clustered multi-hurricane seasons.

Southeast Louisiana is the deltaic Gulf regime: a dense crossing record, strong post-1950 clustering, and prominence in the modern wind-envelope count. Which regime "leads" is a property of the definition, and we have deliberately not combined the definitions into a single weighted score; a defensible composite would require separate hazard models and explicit exposure and vulnerability layers, and this report preserves the physical quantities so that such a model can be built on them transparently.

Two limits of the approach deserve emphasis. Local counting is noisy: Hall and Jewson (2008) scored a basin-wide statistical track model against local landfall counts on 39 coastal segments and found the track model better on 29 of them, but the local model better on the Florida peninsula, on the U.S. Gulf Coast, and on the full coastline taken together, where historical landfalls are frequent enough to constrain the rate; two of our three focal points fall in those groups. Hall and Jewson (2007) note that a different 54-year sample would produce a different landfall profile even in a stationary climate, and Philp et al. (2022), generating counterfactual seasons from ensemble reforecasts, find that the coastal maximum itself moves between plausible histories. Our resampling results quantify that noise for the ranking; they do not remove it. And the climatology is stationary by construction: mean intervals over 126 years average across the multidecadal variability that Keim et al. discuss and the trends examined by Klotzbach et al. (2018), who find no significant trend in continental U.S. landfall frequency over 1900-2017. Time-varying models are the natural extension.

6. Conclusions

Along the U.S. Gulf and Atlantic coasts, hurricane occurrence in 1900-2025 concentrates in south Florida and the Keys, the Outer Banks, and the north-central Gulf Coast, confirming the point climatologies of the last five decades under a different event construction. South Florida is the most probable maximum for hurricane-strength coastline crossings (26 in the optimized neighborhood on the recorded positions, one per 4.85 yr; 69% of season resamples, 45% when landfall-position uncertainty is also admitted, against 28% for southeast Louisiana) and the clear maximum for major-hurricane center passages; the Outer Banks are the most probable maximum for hurricane center passages of any intensity (35, one per 3.60 yr; 63%). Empirical center-proximity intervals run about 0.70 of Keim et al.'s asymmetric-swath values and about 0.74 of NHC's HURISK-modeled values, with rank order preserved in both comparisons. South Florida's seasonal counts are overdispersed, reflecting a tendency toward multi-hurricane seasons with direct implications for preparedness. Stratifying by ENSO reproduces Bove et al.'s phase structure with a current index: La Niña seasons show about twice the strict landfall rate of El Niño seasons. In the modern wind-radii record, hurricane-force envelope exposure has no unique maximum.

Every figure is a historical average over a defined window, not a schedule and not a forecast, and every figure describes occurrence, not risk.

7. Data Availability and Disclosure

Data. HURDAT2 via NOAA/NCEI IBTrACS v04r01 (North Atlantic subset, accessed August 2026); NOAA CPC Relative Oceanic Niño Index; GSHHS/GSHHG shoreline; NOAA/AOML continental U.S. hurricane chronology; NHC-6 Table 12 (Blake et al. 2011); Keim et al. (2007) Fig. 5 return periods (transcribed). All derived tables, the strict landfall catalogue, the bootstrap and comparison outputs, and the complete analysis and figure code are published in the reproducibility package at armorprowindows.com/research, which regenerates every result from the public inputs.

Interest disclosure. Armor Pro Windows & Doors sells and installs impact-rated windows and doors in South Florida and has a commercial interest in public awareness of hurricane exposure. This report was produced and funded internally. It analyzes the public NOAA record with published data and open code; no part of the analysis depends on proprietary data, all analytical choices were fixed before results were examined, and the complete pipeline is published so that any result can be checked independently.

References

Anderson, G. B., J. Ferreri, M. Al-Hamdan, W. Crosson, A. Schumacher, S. Guikema, S. Quiring, D. Eddelbuettel, M. Yan, and R. D. Peng, 2020: Assessing United States county-level exposure for research examining the health effects of hurricanes and tropical storms. *Environ. Health Perspect.*, **128**, 107009.

Blake, E. S., C. W. Landsea, and E. J. Gibney, 2011: The deadliest, costliest, and most intense United States tropical cyclones from 1851 to 2010. NOAA Tech. Memo. NWS NHC-6, 47 pp.

Bove, M. C., J. B. Elsner, C. W. Landsea, X. Niu, and J. J. O'Brien, 1998: Effect of El Niño on U.S. landfalling hurricanes, revisited. *Bull. Amer. Meteor. Soc.*, **79**, 2477-2482.

Chavas, D. R., and K. A. Emanuel, 2010: A QuikSCAT climatology of tropical cyclone size. *Geophys. Res. Lett.*, **37**, L18816.

Chavas, D. R., N. Lin, W. Dong, and Y. Lin, 2016: Observed tropical cyclone size revisited. *J. Climate*, **29**, 2923-2939.

Chenoweth, M., 2014: A new compilation of North Atlantic tropical cyclones, 1851-98. *J. Climate*, **27**, 8674-8685.

Combot, C., A. Mouche, J. Knaff, Y. Zhao, Y. Zhao, L. Vinour, Y. Quilfen, and B. Chapron, 2020: Extensive high-resolution synthetic aperture radar (SAR) data analysis of tropical cyclones: Comparisons with SFMR flights and best track. *Mon. Wea. Rev.*, **148**, 4545-4563.

Dunn, G. E., and B. I. Miller, 1960: *Atlantic Hurricanes*. Louisiana State University Press, 326 pp.

Elsner, J. B., and A. B. Kara, 1997: A climatology of hurricanes for the U.S. Gulf and Atlantic coasts. NOAA Tech. Memo. NWS SR-192.

Elsner, J. B., and A. B. Kara, 1999: *Hurricanes of the North Atlantic: Climate and Society*. Oxford University Press, 488 pp.

Elsner, J. B., K.-b. Liu, and B. Kocher, 2000: Spatial variations in major U.S. hurricane activity: Statistics and a physical mechanism. *J. Climate*, **13**, 2293-2305.

Gelman, A., and P. N. Price, 1999: All maps of parameter estimates are misleading. *Stat. Med.*, **18**, 3221-3234.

Hall, T. M., and S. Jewson, 2007: Statistical modelling of North Atlantic tropical cyclone tracks. *Tellus A*, **59**, 486-498.

Hall, T. M., and S. Jewson, 2008: Comparison of local and basin-wide methods for risk assessment of tropical cyclone landfall. *J. Appl. Meteor. Climatol.*, **47**, 361-367.

Hall, T., and E. Yonekura, 2013: North American tropical cyclone landfall and SST: A statistical model study. *J. Climate*, **26**, 8422-8439.

Ho, F. P., J. C. Su, K. L. Hanevich, R. J. Smith, and F. P. Richards, 1987: Hurricane climatology for the Atlantic and Gulf coasts of the United States. NOAA Tech. Rep. NWS 38, 195 pp.

Ho, F. P., R. W. Schwerdt, and H. V. Goodyear, 1975: Some climatological characteristics of hurricanes and tropical storms, Gulf and East coasts of the United States. NOAA Tech. Rep. NWS 15, 87 pp.

Jagger, T. H., and J. B. Elsner, 2006: Climatology models for extreme hurricane winds near the United States. *J. Climate*, **19**, 3220-3236.

Jagger, T. H., and J. B. Elsner, 2012: Hurricane clusters in the vicinity of Florida. *J. Appl. Meteor. Climatol.*, **51**, 869-877.

Jagger, T. H., J. B. Elsner, and X. Niu, 2001: A dynamic probability model of hurricane winds in coastal counties of the United States. *J. Appl. Meteor.*, **40**, 853-863.

Keim, B. D., R. A. Muller, and G. W. Stone, 2007: Spatiotemporal patterns and return periods of tropical storm and hurricane strikes from Texas to Maine. *J. Climate*, **20**, 3498-3509.

Klotzbach, P. J., 2011: El Niño-Southern Oscillation's impact on Atlantic basin hurricanes and U.S. landfalls. *J. Climate*, **24**, 1252-1263.

Klotzbach, P. J., S. G. Bowen, R. Pielke Jr., and M. Bell, 2018: Continental U.S. hurricane landfall frequency and associated damage: Observations and future risks. *Bull. Amer. Meteor. Soc.*, **99**, 1359-1376.

Knaff, J. A., C. J. Slocum, K. D. Musgrave, C. R. Sampson, and B. R. Strahl, 2016: Using routinely available information to estimate tropical cyclone wind structure. *Mon. Wea. Rev.*, **144**, 1233-1247.

Knapp, K. R., M. C. Kruk, D. H. Levinson, H. J. Diamond, and C. J. Neumann, 2010: The International Best Track Archive for Climate Stewardship (IBTrACS): Unifying tropical cyclone data. *Bull. Amer. Meteor. Soc.*, **91**, 363-376.

Kozar, M. E., M. E. Mann, S. J. Camargo, J. P. Kossin, and J. L. Evans, 2012: Stratified statistical models of North Atlantic basin-wide and regional tropical cyclone counts. *J. Geophys. Res.*, **117**, D18103.

Kulldorff, M., 1997: A spatial scan statistic. *Commun. Stat. Theory Methods*, **26**, 1481-1496.

Landsea, C. W., 2007: Counting Atlantic tropical cyclones back to 1900. *Eos, Trans. Amer. Geophys. Union*, **88**, 197-202.

Landsea, C. W., A. Hagen, W. Bredemeyer, C. Carrasco, D. A. Glenn, A. Santiago, D. Strahan-Sakoskie, and M. Dickinson, 2014: A reanalysis of the 1931-43 Atlantic hurricane database. *J. Climate*, **27**, 6093-6118.

Landsea, C. W., and J. L. Franklin, 2013: Atlantic hurricane database uncertainty and presentation of a new database format. *Mon. Wea. Rev.*, **141**, 3576-3592.

Landsea, C. W., G. A. Vecchi, L. Bengtsson, and T. R. Knutson, 2010: Impact of duration thresholds on Atlantic tropical cyclone counts. *J. Climate*, **23**, 2508-2519.

Merrill, R. T., 1984: A comparison of large and small tropical cyclones. *Mon. Wea. Rev.*, **112**, 1408-1418.

Muller, R. A., and G. W. Stone, 2001: A climatology of tropical storm and hurricane strikes to enhance vulnerability prediction for the southeast U.S. coast. *J. Coastal Res.*, **17**, 949-956.

Neumann, C. J., 1987: The National Hurricane Center Risk Analysis Program (HURISK). NOAA Tech. Memo. NWS NHC-38, 56 pp.

Philp, T. J., A. J. Champion, K. I. Hodges, C. Pigott, A. MacFarlane, G. Wragg, and S. Zhao, 2022: Identifying limitations when deriving probabilistic views of North Atlantic hurricane hazard from counterfactual ensemble NWP re-forecasts. *Hurricane Risk in a Changing Climate*, J. M. Collins and J. M. Done, Eds., Springer, 195-216.

Pielke, R. A., Jr., and R. A. Pielke Sr., 1997: *Hurricanes: Their Nature and Impacts on Society*. Wiley, 279 pp.

Simpson, R. H., and H. Riehl, 1981: *The Hurricane and Its Impact*. Louisiana State University Press, 398 pp.

Simpson, R. H., and M. Lawrence, 1971: Atlantic hurricane frequencies along the United States coastline. NOAA Tech. Memo. NWS-SR-58, 14 pp.

Tartaglione, C. A., S. R. Smith, and J. J. O'Brien, 2003: ENSO impact on hurricane landfall probabilities for the Caribbean. *J. Climate*, **16**, 2925-2931.

Tolwinski-Ward, S. E., 2015: Uncertainty quantification for a climatology of the frequency and spatial distribution of North Atlantic tropical cyclone landfalls. *J. Adv. Model. Earth Syst.*, **7**, 305-319.

Vecchi, G. A., C. Landsea, W. Zhang, G. Villarini, and T. Knutson, 2021: Changes in Atlantic major hurricane frequency since the late-19th century. *Nat. Commun.*, **12**, 4054.

Villarini, G., G. A. Vecchi, and J. A. Smith, 2012: U.S. landfalling and North Atlantic hurricanes: Statistical modeling of their frequencies and ratios. *Mon. Wea. Rev.*, **140**, 44-65.

Wessel, P., and W. H. F. Smith, 1996: A global, self-consistent, hierarchical, high-resolution shoreline database. *J. Geophys. Res.*, **101**, 8741-8743.

Wilks, D. S., 2016: "The stippling shows statistically significant grid points": How research results are routinely overstated and overinterpreted, and what to do about it. *Bull. Amer. Meteor. Soc.*, **97**, 2263-2273.